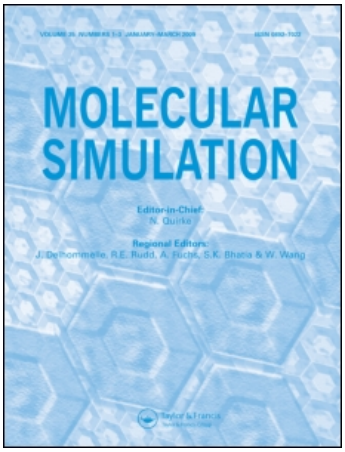

Molecular Simulation
Publication details, including instructions for authors and subscription information:
http://www.informaworld.com/smpp/title~content=t713644482

The conductor-like screening model for polymers and surfaces

B. Delley[a]
[a] Paul Scherrer Institute Switzerland, Villigen, Switzerland

To cite this Article Delley, B.(2006) 'The conductor-like screening model for polymers and surfaces', Molecular Simulation, 32: 2, 117 — 123
To link to this Article: DOI: 10.1080/08927020600589684
URL: http://dx.doi.org/10.1080/08927020600589684

Molecular Simulation, Vol. 32, No. 2, 15 February 2006, 117–123

Taylor & Francis
Taylor & Francis Group

The conductor-like screening model for polymers and surfaces

B. DELLEY*

Paul Scherrer Institute Switzerland, Villigen CH-5232, Switzerland

(Received November 2005; in final form January 2006)

The DMol^3 COSMO method is revisited and generalized for infinite polymer and surface models with periodic boundary conditions. The procedure works also for three dimensionally periodic solid models with internal surfaces. A new solvent accessible surface grid construction is presented, where the grid points and weights are a continuous function for all atomic geometries. The calculated solvation energy is also continuous by consequence, which is useful for all calculations which involve geometry changes of the atomic framework. The new method is tested with a few examples.

Keywords: COSMO; Solvation model; Periodic boundary conditions; Density functional theory

1. Introduction

Continuum solvation models, in particular the conductor-like screening model (COSMO), are well established methods to incorporate solvation effects into quantum chemical calculations. The results from the COSMO calculation are typically used in the COSMO-RS model [1] which delivers astonishingly accurate predictions for the thermodynamic properties of mixtures. In this work, the DMol COSMO method [2] is revisited and generalized for periodic boundary conditions. The periodic boundary conditions allow quantum calculations of infinite systems in one to three dimensions, and can be applied to polymers, surfaces and also to internal surfaces in solids. Indeed, solvation energies for polymers have already been estimated based on calculations for finite length chain molecules. The solvation part could be extracted either by extrapolation or by cutting out the part of the repeat unit. The question about the influence of the end groups is hard to address, and here the ideal model with periodic boundary conditions makes a clean case. For surfaces, the issue with the termination of a cluster model is much more pressing than in the polymer case. The termination dramatically alters the density of states when comparing a cluster model with an infinite model. In the case of a metallic surface, there is even a qualitative difference, in that the cluster model necessarily has a non-metallic density of states. Since, the orbital energies are derivatives of the total energy with respect to occupation numbers, the spurious energy gaps present in the cluster model are suggestive of the energy errors that can occur for reaction energies.

The present work is focused at the generalization of the COSMO method to the periodic boundary case. The desirability of a continuous dependence of the energy as a function of atomic positions especially for vibrational and first principles molecular dynamics calculations has lead to a minor redesign of the cavity construction and a major redesign of the discretization of the cavity. Implications of three dimensional periodicity make it desirable to localize exactly all of the screening charge at the cavity surface, which is achieved here with a Lagrange constraint. The cavity discretization is also connected with the calculation of electrostatics. The current simplified approach is sketched in the methods section.

The present revised DMol^3-COSMO method is tested for its performance in the COSMO-RS benchmark set. The results suggest that a small improvement against the previous method has been achieved. Somewhat, preliminary tests are also shown for two polymers and two surfaces. The perfect feasibility of such calculations is obvious. Currently, however, a benchmark set for polymers and surfaces is missing, which would allow a statistical statement on the accuracy to be expected.

*E-mail: bernard.delly@psi.ch

Molecular Simulation
ISSN 0892-7022 print/ISSN 1029-0435 online © 2006 Taylor & Francis
http://www.tandf.co.uk/journals
DOI: 10.1080/08927020600589684

2. Method

The DMol^3 method [3,4], originally a method for density functional theory (DFT) calculations of molecular clusters in the gas phase, was generalized early on [2] to model a solvent environment of a molecule via the COSMO [5]. This method involves the construction of a solvent accessible surface (SAS) and the solution of electrostatics related to the screening charges located at the SAS. This SAS grid construction, referred to here as "Klamt", has small discontinuities when atoms move. This is an important reason to consider an alternate SAS construction here. It is desirable to not introduce discontinuities in the energy surface when aiming at optimizations, vibrational calculations and DFT molecular dynamics. An issue with any SAS is with the charge associated with the orbital tails falling outside the SAS. A small non variational correction term for COSMO has been introduced by Klamt and Jonas [6]. We use the abbreviation OC for their outlying charge correction.

The SAS is primarily defined via element dependent radii, which are parameters optimized for the COSMO-RS model. Typically, the values are about 17% larger than the Van der Waals radii. One is lead to consider a surface with the crevices between the atomic spheres filled in [1]. In the present work, the SAS is defined as the iso-surface $F(\mathbf{r}) = 0$, which is a continuous and fast to evaluate function of the atomic positions. The function F embodies a sort of ball and stick model. It is expedient to define an auxiliary function

$$f(x) = -\mathrm{e}^{-\alpha x} + ax + bx^2$$

with a sharpness parameter α. The auxiliary parameters a and b are derived from the conditions $f(x_c) = 0, \quad f'(x_c) = 0$ with $x_c = 4/\alpha$. $f(x)$ is essentially the function $-\exp(-\alpha x)$ in the region of interest. The purpose of the cut off is fast, O(N), evaluation without introducing a discontinuity for the iso-surface. F can now be defined as

$$F(\mathbf{r}) = 1 + \sum_i f\left(\left((\mathbf{r} - \mathbf{r}_i)^2 - R_i^2\right)\right)/(2R_s R_i)) + \sum_{i \neq j} f\left(\left((\mathbf{r} - \mathbf{r}_z(ij))^2 - R_z^2(ij)\right)/(2R_s \max(R_z, 1a_0))\right).$$

where $\mathbf{r}_i$ are the atomic positions and R_i are the SAS radii. $F(\mathbf{r})$ is a function that takes the value zero at the COSMO surface, deep inside the enclosed surface F has large negative values. On going through the surface from the inside, F behaves like $1 - \exp(-\alpha(r - R_i)/R_i)$. The third term in F relates to the capped stick part of the model. $\mathbf{r}_z(ij)$ is the projection of $\mathbf{r}$ onto the bond line, if this falls between the atomic positions i,j, else $\mathbf{r}_z(ij)$ is limited to the atomic position at the end in question.

$$R_z(ij) = \left(S_i^2 - \left(\frac{S_i^2 + d_{ij}^2 - S_j^2}{2d_{ij}}\right)^2\right)^{\frac{1}{2}} - R_s$$

is the radius of the cylinder that is touched a sphere of radius R_s which also touches spheres R_i and R_j. The distance of the center of this R_s sphere from the atomic center i is $S_i = R_i + R_s$. We use $R_s = R_H$, the same as the hydrogen SAS parameter. d_{ij} is the distance between i and j. Stick contributions are dropped when $d_{ij} > S_i + S_j$. This iso-surface varies continously with the atom positions. The sharpness parameter α smoothes the sharp edges where two or more spheres or cylinders meet. For too small values of α, the SAS surface becomes obese and the dielectric screening energy is lowered. A value of $\alpha = 50$ leads to consistently good results, the exact value is not critical. The gradient of the function F defines the surface normal.

The SAS can be modified by user defined exclusion or spacer spheres which are treated like additional atoms. The main purpose is to prevent a spurious SAS appearing in an internal void of the compound.

For COSMO, it is necessary to evaluate integrals over this surface. To generate integration grids on this surface, integration grids for the unit sphere [7] are radially projected out to the surface from each atomic center. The SAS parts are assigned to the atomic centers according to the planes through the intersection circles of the SAS spheres. For nonintersecting spheres, the dividing plane, normal to the bond, is positioned such that the distance of the plane to the nuclei is proportional to the SAS parameters. Weights belonging to integration points projected onto the bond part of the surface, are scaled according to the skew projection onto the touching plane at the perforation point of the projection vector. The weight is interpreted as an area of elliptical shape. If the ellipse is intersected by a dividing plane, the fractional area of the ellipse, on the side of the atom owning the integration point, is evaluated along with the center of gravity of the fractional area. The integration point position is set to the center of gravity, and thus remains on the owner-atom side of the divide even if the original point was not. The weight is adjusted according to the fractional area. Points with zero area on the owner atom side correspondingly have zero weight and can be discarded. Point positions and weights are a continuous function of the atomic positions by this construction. The integration grids on the unit sphere achieve high order convergence for smooth functions. While the exact COSMO problem would lead to functions obeying such continuity conditions, the present SAS surface grid does not have these high order convergence properties. This is not a problem in practice, since these errors are much smaller than the ones from the COSMO models applied to real solvents. A sufficient level of convergence is reached using a 110 point scheme [7] for all atoms except hydrogen, where the 50 points scheme is used. This scheme (ibs 110-50) is adopted as the default scheme. This mesh size is similar to the 92-32 icosahedral meshes used in the original Klamt method.

The issue of missing screening charge can be addressed in a variational way. The charge on the SAS is constrained to contain exactly the opposite charge of the solvated compound including its tail charge. This is done by extending the dielectric energy formula by a Lagrange

constraint term,

$$E_{\text{diel}} = QBq + 1/2qAq + \Phi(Q_{\text{net}} + \Sigma q)$$

The first two terms represent the discretized solvent part of the electrostatic energy written in matrix notation as in previous work. q is the vector of the screening charges on the surface of the cavity, Q the charges of the solute comprised of the electronic and nuclear charges. Q_{net} is the net charge of the molecule. B is the Coulomb interaction of the solute and the screening charges. A is the electrostatic interaction among the screening charges. Σ can be seen as vector with all elements equal to 1, producing the sum of charges via the scalar product. The total solvation energy at the COSMO level includes a term from the quantum part $E_{\text{solv}} = E_{\text{t}}(q) - E_{\text{t}}(q = 0) + E_{\text{diel}}$, where E_{t} is the total energy in the presence/absence of COSMO screening. The condition for stationarity with respect to the screening charges is

$$QB + qA + \Phi\Sigma = 0.$$

The interaction energy for the stationary values q_0 is:

$$E_{\text{diel}} = -1/2q_0Aq_0 + \Phi\Sigma q_0.$$

In the case of neutral solutes, $\Sigma q_0 = 0$ and the second term vanishes. For charged molecules, but hypothetically with all of Q enclosed by the SAS, the constraint would correct only for discretization errors. In the fully converged limit, discretization errors go to zero and with it the value of the Lagrange parameter for the "enclosed charge" case.

Special attention has to be paid to the near field electrostatics for the discretized electrostatics embodied in matrices A and B. Here, the approximate near field formula for a disc of radius r_{s} is used: $A_{ij} = (2 - d_{ij}/r_{\text{s}})/r_{\text{s}}$, with $r_{\text{s}} = \max(r_{si}, r_{sj})$. The maximum property of r_{s} is mainly for completeness of the definition, since with the exception of the diagonal term $d_{ij} = 0$ there remain very few other near field pairs i,j. The same formula applies for the solute—COSMO cavity interaction $B_{ij} = (2 - d_{ij}/r_{\text{s}})/r_{\text{s}}$.

The generalization of the COSMO models to periodic structures can be done by the same methods as for the quantum mechanical and associated electrostatic part of the DFT calculation. For DMol^3, the lattice periodic electrostatics is done by the Ewald method [8]. For polymers and surfaces, the structures are periodically repeated in three dimensions. The minimum separation between periodically repeated structures is given by the condition that the overlap matrix element for the localized basis functions should vanish between the periodic images. The condition can be formulated as $C_z > z_{\max} - z_{\min} + 2{*}r_{\text{cut}}$, where C_z is the lattice translation vector normal to the surface. $z_{\max}, z_{\min}$ are the max and min components of the coordinates normal to the surface for the atoms in the slab. r_{cut} is the radial cutoff for the relevant basis function in the quantum part of the calculation. The minimum requirement for the separation of the periodic replicas arising from COSMO is that the SAS should not be modified by the neighbor. This leads to $C_z > z_{\max} - z_{\min} + 2{*}r_{\text{COSMO}} + 2{*}R_{\text{s}}$, where r_{COSMO} is the relevant COSMO parameter for elements at the surface. Usually this COSMO condition is more permissive than the condition shown first. This means that the same repeat vectors may be used without or with a COSMO part in the calculation.

3. Test and applications

3.1 Theoretical and computational details

All calculations were performed using the DMol^3 method [3] for DFT calculations. The method applies to calculations for isolated molecular clusters with vacuum boundary conditions as well as for band structure calculations with periodic boundary conditions. For solids, reciprocal space meshes and tetrahedron methods are automatically available for a proper sampling of the orbitals across the Brillouin zone. For the present work, the DNP basis set is used throughout. This basis set has been shown to give energy differences close to the DFT basis set limit [9]. If not, otherwise, indicated the PBE functional [10] was used. For some calculations, the BP functional is used, a combination of "Becke 88" exchange [11] and "Perdew 91" correlation [12]. A few other calculations were done with the basic local density functional PWC [13]. For the other settings, the DMol^3 default values were used, unless noted specifically.

3.2 Molecular tests

Molecular tests were done using the COSMO-RS database with experimental values for ΔG of hydration, the log of vapor pressure and of partition coefficients for mixtures where known. This database contains data for 290 molecules with a total of 1134 benchmark values available. Evaluation was done by taking the standard deviation of COSMOtherm predictions for the benchmark values using optimized COSMO-RS parameters. The idea behind this type of test is that the hydration energy from the COSMO model is of limited interest and significance. An interesting part of the result is contained in the screening charge distribution function, the sigma profile, for each species. The partly empirical COSMO-RS method uses all of this information to make improved predictions for a variety of thermodynamic properties involving liquids. The results of this test are summarized in table 1.

The main result is that the new COSMO procedure introduced here, because of the needs of calculations with periodic boundary conditions, shows similar, if not better, consistency of results as previous parametrizations. Not shown are results for finer grids of the new type. The performance is just the same for finer grids, even with ten times more grid points. This suggests that the coarseness

Table 1. Performance of COSMOtherm predictions for benchmark values when parametrized for the specific COSMO model.

Method	*Functional*	*Grid*	*Perf. [kcal/mol]*
DMol[3]	PBE	Present: ibs	0.355
DMol[3]	PBE	Klamt* Lagr	0.359
DMol[3]	PBE	Klamt + OC[†]	0.362
DMol[3]	BP	Klamt + OC	0.377
TURBOMOLE[‡]	BP	Klamt + OC	0.396
DMol[3]	PWC	Present: ibs	0.372

Lagr refers to the Lagrange constraint introduced in this work. 1 kcal/mol = 4.184 kJ/mol;[*] Ref. [1]. [†] Ref. [1,6]. [‡] Ref. [14].

of the default grid is not limiting the accuracy of the models. The entry "Klamt Lagr" uses the Lagrange method to localize the integrated screening charge on the SAS. This leads to almost identical results as the original Klamt method with outlying charge corrections. The performance shown here is in support of this very close similarity. Finally, these data show a small effect due to the functional approximations and the default basis sets used here.

The ibs grid leads to surface areas which are in very close agreement at the 1% root mean square (RMS) level with the ones from the Klamt method. The grid areas are converged at the 1% level when compared to the fine grid calculations. Solvation energies from the ibs method turn out slightly smaller than with Klamt's method including outlying charge corrections. Already, the 'Klamt Lagr' method leads to slight reduction of the COSMO solvation energy. The ibs grid leads to a further slight reduction of COSMO solvation energy. The OC type of correction is not available for the ibs grid. Figure 1 shows scatter-plots for COSMO dielectric energies across the database for different methods. Most of these differences are compensated in the RS parametrization, and will not impact on thermal modeling when the proper parameters are used. The dielectric energies of the standard ibs model are in excellent agreement with the finest grid ibs calculations.

3.2 Polymer models

Polymer models are studied here mainly to demonstrate the feasibility of such calculations and the actual functioning of the code. The solvation energy is naturally calculated per structural unit that was defined as the repeat unit. A *N*-acetyl-Gly-Gly-C-methylamine structure has been chosen by Cossi [15] as the reference monomer to be compared with an infinite glycine chain. The quantum part was replaced by static charges in the test calculations by Cossi. Our present calculations use the full DFT quantum model. The default only provides 2 k-points for reciprocal space integrations of orbitals along the chain direction. This is converged to better than 0.01 kcal/mol for the solvation energy.

For the glycine "monomer", the end groups contribute more to the solvation energy than the repeat unit. This is intuitively clear from figure 2 showing the "monomer" and the polymer unit with the finest COSMO ibs grid. The points are colored according to the averaged charges as used for the σ-profiles. In the case of thiophene, the end groups consist in just H atoms, while the repeat unit in poly-thiophene consists of two ring units. While the COSMO solvation energies for thiophene monomer and polymer look very similar, again the end group produces about half of the solvation energy for the monomer.

Polymers have a well defined volume per repeat unit, but the volume of the entire polymer string has a large value and tends to infinity in the idealization of the periodic boundary conditions. We expect that mixtures involving polymers can be treated ultimately in a similar semiempirical COSMO-RS [1] solvent model as small

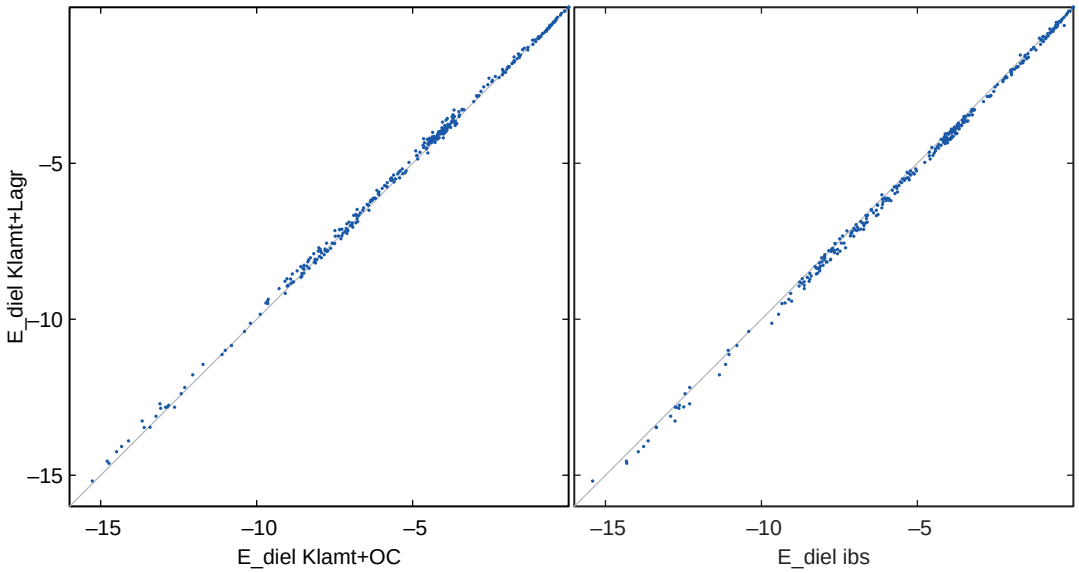

Figure 1. Scatter plots for the comparisons of COSMO dielectric energy for the 290 test molecules. (a) Klamt + Lagr vs ibs method and (b) Klamt + Lagr vs Klamt + OC method. Plots in units of 1 kcal/mol = 4.184 kJ/mol.

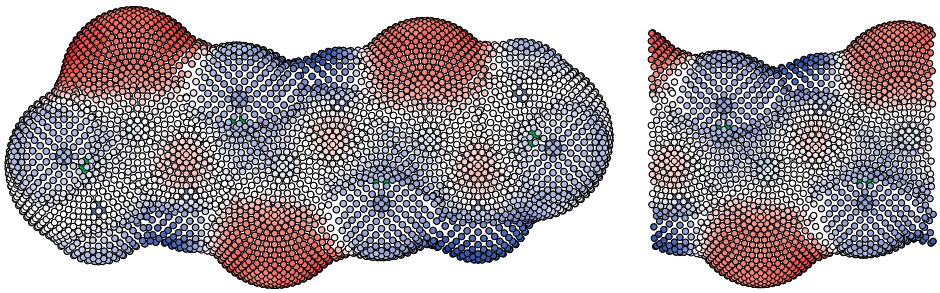

Figure 2. Glycine "monomer" (*N*-acetyl-Gly-Gly-C-methylamine) and poly-glycine with charges on the SAS for the finest ibs grid. Color code for charges, blue $-2\,e/nm^2$, red $+2\,e/nm^2$ and white zero, the pictured area of the charge disks does not represent the actual size.

molecules. For this type of simulation, the quantum calculations presented here can provide the σ-profile needed. As an example, the σ-profile of poly-glycine is shown in figure 3. If it is assumed that a charge density of $1\,e/nm^2$ on the COSMO solvent accessible surface marks the divide between weak and strong hydrogen bonding (page 86 [1]), it is quite obvious from the figure that poly-glycine does contain a stronger polar positive screening charge and a weakly polar negative screening charge. The comparison of the standard mesh result with the result from the fine mesh 1202 − 434 shows that the salient features of the profile are well captured at the standard level. The benchmark calculations for the molecules suggest that the improved convergence with the ten times finer mesh does not entail a significant improvement for the prediction of thermodynamic properties. This observation is of some importance for practical calculations, since with the periodic boundary conditions, the COSMO part becomes a larger fraction of the computational cost (table 2).

3.4 Surfaces

Electrostatic screening of polar surfaces may be of interest as a model for heterogeneous catalysis involving a liquid phase. A first surface being studied here is the hydroxylated α-quartz (0001) surface. A minimalistic slab model is used which is based on an α-quartz conventional cell. The cell composition is $H_2O{-}(SiO_2)_n{-}OH_2$ (see figure 5) Energy minimization turns the hydroxyl groups into the plane with hydrogen pointing to the nearest other oxygen atom, forming a regular array of hydrogen bridges. These hydrogen bridges also form in the presence of the COSMO screening. For macroscopic considerations of surface energy, the atomic roughness is disregarded. The planar area can be deduced from the two dimensional translation vectors along the surface. With the slab model both, the front and back, surfaces constitute solvent accessible areas. In the present cases of interest, the front and back surface are symmetry equivalent and lead simply to a duplication of surface area. Hydroxyl terminated quartz has a fairly wide sigma profile, which leads to quite important interfacial energies with a high dielectric liquid. This is evidenced by the σ-profile for the quartz surface shown in figure 4. The width of the sigma profile of the thin slab model is significantly less wide than for more realistic thicker slab models.

The SAS surface is shown in figure 5. The surface is quite strongly corrugated. Without the bond part in the ibs construction of the SAS, the surface would reach far inside the slab, requiring eg an exclusion sphere to make such a model work. It is a bonus of the ibs model that for most surfaces no exclusion spheres will be needed. Still, some solids, such as ice, C^{60}, have such large internal voids that exclusion spheres are required to suppress spurious SAS. In the case of zeolites, another class of solids with large voids, one may consider modeling the liquid in the void by

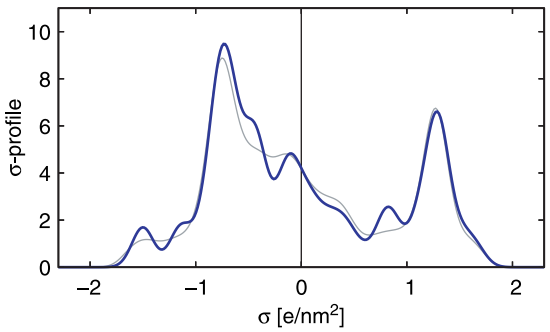

Figure 3. Poly-glycine σ-profile sharp line with standard discretization, wide line with fine discretization of the ibs 1202 − 434 grid.

Table 2. COSMO solvation free enthalpies in kcal/mol for glycine and thiophene polymers per repeat unit, and for the corresponding monomer units with termination.

Method	*Functional*	*Grid*	*Monomer*	*Polymer*
Glycine polymer				
DMol[3]	PBE	Present: ibs	−22.72	−10.39
DMol[3]	PBE	ibs 194 − 110	−22.48	−10.24
DMol[3]	PBE	ibs 302 − 110	−22.25	−10.12
DMol[3]	PBE	ibs 590 − 194	−22.24	−10.13
DMol[3]	PBE	ibs 1202 − 434	−22.11	−10.05
DMol[3]	PBE	Klamt* + OC[†]	−22.92	−10.28
Cossi[‡]	–	GEPOL	−20.63	−8.85
Poly-thiophene				
DMol[3]	PBE	Present: ibs	−3.71	−3.74
DMol[3]	PBE	ibs 590 − 194	−3.74	−3.80
DMol[3]	PBE	ibs 1202 − 434	−3.72	−3.79
DMol[3]	PBE	Klamt* + OC[†]	−4.14	−4.42

[*] Ref. [1]. [†] Ref. [1,6]. [‡] Ref. [15].

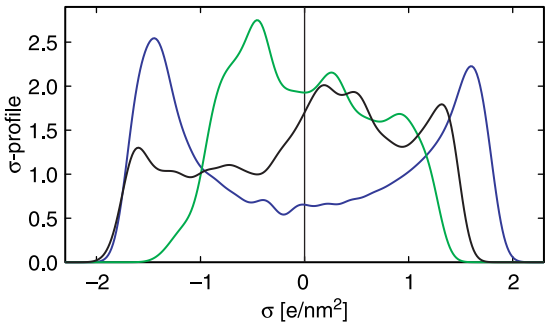

Figure 4. σ-profiles for hydroxylated α-quartz (0001) slab $d = 0.6$ nm green, slab $d = 3.2$ nm black compared to H_2O blue, all calculated with ibs 1202 − 434 grid.

COSMO. The present method is technically up to such a treatment. The merits of COSMO for internal wetting in zeolites remains to be investigated.

We have also studied the liquid–solid interfacial energy of α-sulfur (001), using a slab cell containing two conventional cells of the bulk. This slab has the composition $(S_8)_n$. The COSMO interfacial energy turns out small as expected, and the surface is essentially nonpolar.

The surface energy is the energy gain by wetting the surface. It is clear that wetting is a complex phenomenon showing hysteresis, pinning of the contact line, etc. [16]. At the most basic level, static wetting is described by Young's law: $\gamma_{SL} - \gamma_{SV} + \gamma\cos(\theta) = 0$, where γ_{SV} is the surface energy of the solid against the gas phase, and γ_{SL} against the liquid. γ is the surface tension of the liquid.

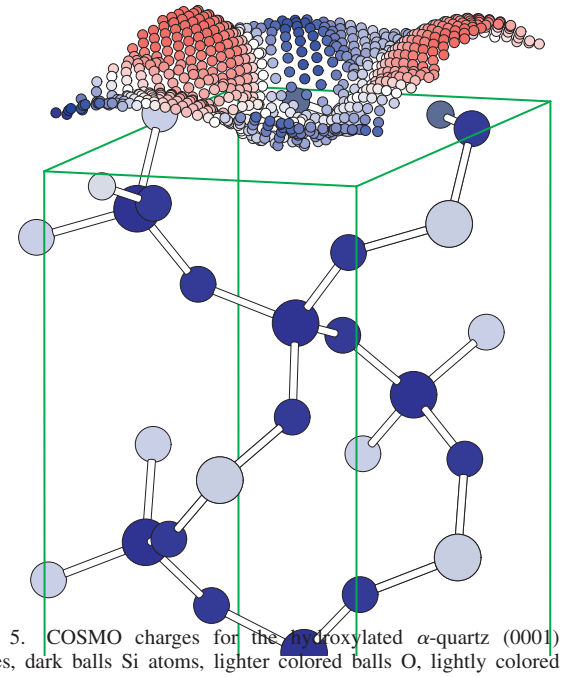

Figure 5. COSMO charges for the hydroxylated α-quartz (0001) surfaces, dark balls Si atoms, lighter colored balls O, lightly colored balls: atoms in adjacent cells involved in bonds with the atoms in the cell. Color code for COSMO charges, blue -2 e/nm^2, red $+2$ e/nm^2 and white zero. Upper half of slab is shown, face of cell indicates atomic surface plane.

At the COSMO level $\Delta\gamma = \gamma_{SL} - \gamma_{SV} = E_{solv}/A_c$, the "solvation energy" per planar surface area A_c. In a slab model, A_c usually refers to the combined area from both sides of the slab. On the experimental side, contact angle measurements are an important tool to study liquid–solid interfacial energies. With Young's law, one has $\Delta\gamma = -\gamma\cos(\theta)$. To convert the experimental contact angles from [17] to $\Delta\gamma$, the experimentally well known surface tension of water $\gamma = 72.8$ mN/m is used. The discrepancy of the present COSMO surface energies with the experimentally deduced values in table 3 looks uncomfortably large when expressed in mN/m units. It is not clear at present what may be the cause of the discrepancy. It could be that the ideal surface is much smoother than the real surface. It could also be that long range terms not present in the COSMO model significantly contribute to the interfacial energy. Finally, the experimental surface is specified by the preparation procedures and is possibly not the face assumed here. The idealized model here may also miss reconstruction modes of relevance. For the α-quartz slab, there appear to be geometrically minor relaxations deep into the slab, however, with significant effect on the dielectric energy. Consequently, thinner quartz slab models show less dielectric energy gain than thicker ones. As these issues have not been explored for now, the present wetting energies should be considered as preliminary results.

3.5. Summary and conclusion

The DMol^3 COSMO method has bee revisited and extended to periodic boundary conditions for polymer and surface models. A new method to define the solvent accessible surface was introduced which leads to continuous variation of all properties as a function of geometry. This is desirable in geometry optimizations, vibrational and *ab-initio* molecular dynamics calculations. The newly introduced Lagrange method for localizing the screening charge on the solvent accessible surface is variational. Moreover, the need for an outer surface, as needed for the previously introduced OC corrections, is obviated. The new methods lead to a slight improvement for COSMO-RS predictions for the COSMOtherm benchmark data set. We have also shown demonstration applications to polymers and surfaces. The generalization for solvation from molecules to polymers is mostly straightforward. Only the volume term in the COSMO-RS model may require more thought, as the entire idealized polymer molecule has an infinite volume. The generalization to surfaces may open a new field in modeling liquid–solid interfaces. The slab model preserves a qualitatively correct description of the electronic structure of the solid. The chemistry at the liquid–solid interface, can now be modeled by keeping as many, or few, molecules as needed and the rest of the liquid incorporated into the COSMO model.

Table 3. COSMO liquid–solid interfacial energies for $\epsilon = \infty$ liquid.

Method	*Functional*	*Surface*	*n*	*d [nm]*	A_2 *[nm^2]*	ΔG_{diel} *[kcal/mol]*	$\Delta\gamma$ *[mN/m]*	$\Delta\gamma$ *exp [mN/m]*
DMol^3	PBE	α-quartz (0001)	3	0.6	0.418	−1.94	−32.3	
DMol^3	PBE	α-quartz (0001)	9	1.7	0.418	−3.32	−55.2	
DMol^3	PBE	α-quartz (0001)	17	3.2	0.418	−3.54	−58.8	−61.1
DMol^3	PBE	α-sulfur (001)	8	2.5	1.346	−0.88	−4.6	−11.3

n, number of formula units (SiO_2 respectively S_8) in the slab cell; d, slab thickness; A_2, surface cell area for front and back side of slab; ΔG_{diel}, per slab cell; $\Delta\gamma$, dielectric energy per area, exp from contact angles in [17].

Acknowledgements

The author thanks A. Klamt and F. Eckert for stimulating discussions and for help with COSMO-therm benchmarks.

References

[1] A. Klamt. *COSMO-RS, from quantum chemistry to fluid phase thermodynamics and drug design*, Elsevier, Amsterdam (2005).
[2] J. Andzelm, Ch. Kölmel, A Klamt. Incorporation of solvent effects into density functional calculations of molecular energies and geometries. *J. Chem. Phys.*, **103**, 9312 (1995).
[3] B. Delley. An all-electron numerical method for solving the local density functional for polyatomic molecules. *J. Chem. Phys.*, **92**, 508 (1990).
[4] B. Delley. From molecules to solids with the DMol^3 approach. *J. Chem. Phys.*, **113**, 7756 (2000).
[5] A. Klamt, G. Schüürmann. COSMO: a new approach to dielectric screening in solvents with explicit expressions for the screening energy and its gradient. *J. Chem. Soc. Perkin Trans.*, **2**, 799 (1993).
[6] A. Klamt, V. Jonas. Treatment of the outlying charge in continuum solvation models. *J. Chem. Phys.*, **105**, 9972 (1996).
[7] B. Delley. High order integration schemes on the unit sphere. *J. Comput. Chem.*, **17**, 1152 (1996).
[8] B. Delley. Fast calculation of electrostatics in crystals and large molecules. *J. Phys. Chem.*, **100**, 6107 (1996).
[9] B. Delley, R.D. Johnson to be published. HTTP://num.web.psi.ch/reports/2004/CMT/cmt-2004-01.pdf.
[10] J.P. Perdew, K. Burke, M. Ernzerhof. Generalized Gradient Approximation Made Simple. *Phys. Rev. Lett.*, **78**, 3865 (1996).
[11] A.D. Becke. Density-functional exchange-energy approximation with correct asymptotic behavior. *Phys. Rev. A*, **38**, 3098 (1988).
[12] Y. Wang, J.P. Perdew. Correlation hole of the spin-polarized electron gas, with exact small-wave-vector and high-density scaling. *Phys. Rev. B*, **44**, 13298 (1991).
[13] J.P. Perdew, Y. Wang. Accurate and simple analytic representation of the electron-gas correlation energy. *Phys. Rev. B*, **44**, 13244 (1992).
[14] Frank Eckert private communication.
[15] M. Cossi. Continuum solvation model for infinite periodic systems. *Chem. Phys. Lett.*, **384**, 179 (2004).
[16] P.G. de Gennes. Wetting: statics and dynamics. *Rev. Mod. Phys.*, **57**, 827 (1985).
[17] A. Sklodowska, M. Wozniak, R. Matlakowska. The method of contact angle measurements and estimation of work of adhesion in bioleaching of metals. *Biol. Proc. Online*, **1**, 114 (1999).